Nonwoven electrowetting textiles

K. Bhat and J. Heikenfeld[a)]
Novel Devices Laboratory, Department of Electrical and Computer Engineering, University of Cincinnati, Cincinnati, Ohio 45221

M. Agarwal, Y. Lvov, and K. Varahramyan
Institute for Micromanufacturing, Louisiana Tech University, Ruston, Louisiana 71272

(Received 25 April 2007; accepted 10 June 2007; published online 11 July 2007)

Electrowetting of two nonwoven textile platforms is reported. Demonstrated nonwoven textiles include a polyethylene naphthalate film that was laser milled with ~125 μm pores, and pressed paper that was made using wood microfibers of 35–50 μm diameter. Vacuum deposition provided an Al electrode on the polymer textile whereas layer-by-layer nanoassembly provided an organic PEI-PEDOT:PSS electrode on the wood microfibers. Both textiles were electrically insulated with parylene C and fluoropolymer. Irreversible electrowetting of water was achieved over contact angles of ~120° to ~70° by applying 0–100 V. Completely reversible electrowetting of water/oil was also demonstrated. © *2007 American Institute of Physics*. [DOI: 10.1063/1.2753750]

The dominant paradigm in textile manufacturing is that wetting properties are permanently determined at the time of manufacturing. However, there are an increasing number of approaches that allow surface wetting to be modulated in real time at the end-user level. Several techniques for wetting modulation include optically reconfigured spiropyrans,[1] thermocapillarity,[2] redox-active surfactants,[3] and electrowetting.[4] Electrowetting is seeing rapid growth as it is enabling potentially important fluidic technologies for lab on a chip,[5,6] liquid optics,[7,8] and high brightness displays.[9,10] In this letter, we report on electrowetting applied to nonwoven textiles. Fabrication of polymer and wood microfiber electrowetting textiles is described. A brief review of electrowetting theory on nonplanar surfaces is provided along with experimentally observed results for electrowetting textiles. Lastly, textile electrowetting with colored oil and water is presented as a basis for improved reversibility and for tunable color surfaces.

An electrowetting textile could be considered as a specialized class of electrotextile.[11] Like many general electrotextiles, electrowetting textiles require an integrated conductor and a conformal electrical insulator. An electrowetting textile further requires a hydrophobic surface so that a wide range of wetting modulation may be achieved. Taking these criteria into consideration, fabrication of the electrowetting textiles shown in Fig. 1 was performed as follows. Nonwoven scaffolds were chosen over a woven bicomponent[12] fiber scaffold since nonwoven fibers are immobilized and less susceptible to fiber-to-fiber abrasion. Nonwoven polymer textiles were fabricated by CO_2 laser milling of holes in a ~125 μm thick polyethylene naphthalate (PEN) film. Several samples were fabricated with hole radii of ~50 μm and hole densities ranging from approximately tens to thousands of holes/cm^2. This nonwoven PEN textile was then cleaned and a 50 nm coating of Al was deposited onto the textile. The textile was then coated with ~1 μm of parylene C using a Speciality Coating Systems 2010 lab coater. Parylene C provides pinhole-free electrical insulation (2 MV/cm, ε_r ~3) and conformal coating even for nanoscale features.[13] The samples were then dip coated with a fluoropolymer solution. The dip-coating solution consisted of 1 wt % DuPont Teflon AF fluoropolymer in 3*M* FC-40 fluorosolvent. The low 16 mN/m surface tension of the solution allows for permeation and coating of the pores in the textile. Next, the textile was baked at 120 °C for 15 min and a final surface energy of ~16–18 mN/m was obtained. The fluoropolymer thickness was approximately hundreds of nanometers with some thickness variation due to dip coating onto a nonplanar surface. The combined parylene/Teflon film stack is herein referred to as the hydrophobic dielectric. A second nonwoven textile was fabricated from pressed wood microfibers (lignocellulose) that are ~3 mm in length and 35–50 μm in diameter. A layer-by-layer nanoassembly of conducting poly(3,4-ethylenedioxythiophene)-poly(styrenesulfonate) (PEDOT-PSS) polymer on wood microfibers was utilized to make the fibers and textile electrically conductive.[14,15] Polycation poly(ethyleneimine) (PEI) was deposited in alternate sequence with the anionic PEDOT-PSS to construct an electrostatically connected multilayer on the wood microfibers. The four bilayers of PEI and PEDOT-PSS were optically measured to have a total coating thickness of 30 nm. The moderate conductivity achieved (~1–10 S/cm) for the

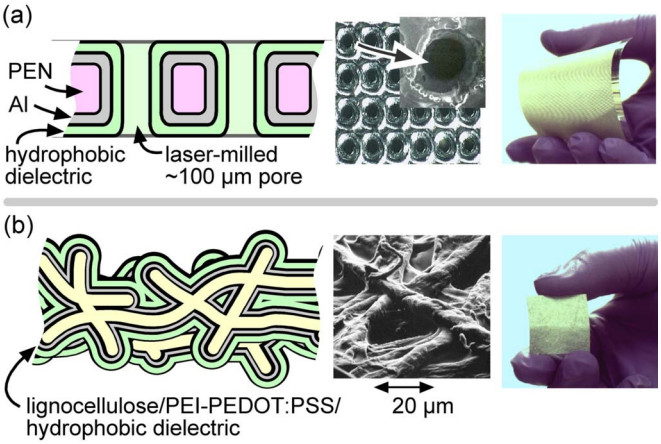


FIG. 1. (Color online) Diagrams, SEM images, and optical images, of electrowetting textiles based on (a) PEN and (b) wood microfibers.

[a)]Electronic mail: heikenjc@email.uc.edu

 © 2007 American Institute of Physics
Downloaded 25 Jan 2008 to 129.137.215.236. Redistribution subject to AIP license or copyright; see http://apl.aip.org/apl/copyright.jsp

PEI-PEDOT:PSS coated microfibers is adequate for electrowetting modulation since electrowetting only requires capacitance charging and does not require dc current flow. This microfiber textile was then electrically insulated with parylene C and made hydrophobic with Teflon AF coating using the procedures previously described for the PEN textile. Images of the fabricated textiles are shown in Fig. 1. It can be noted from Fig. 1 that the PEN textile was highly flexible, whereas the microfiber was flexible, but subject to creasing for bend radii below a few centimeters. Liquids for electrowetting testing included de-ionized water or 0.1*M* KCl saline solution ($\gamma \sim 73$ mN/m). Contact angles were measured using an AST VCA-Optima system. The difference in advancing and receding contact angle was measured to be $\sim 20°$ for the PEN textile and $\sim 40°$ for the microfiber textile. For all electrowetting experiments, the liquids were grounded and the electrical potential was applied to the textiles.

Electrowetting occurs as applied voltage results in charge accumulation near the three-phase liquid/solid/ambient contact line.[4] This charge accumulation alters the balance of interfacial surface tension forces and reduces the liquid contact angle. The textile surfaces presented here are highly irregular compared to other reports of planar[4] or structured[16,17] electrowetting surfaces. However, as a first approximation electrowetting on a textile may be predicted by the Cassie and Baxter equation [Eq. (1a)] and the so-called electrowetting equation [Eq. (1b)] adapted to a planar surface with voids,[18]

$$\cos \theta_S = \beta(1 + \cos \theta_Y) - 1, \tag{1a}$$

$$\cos \theta_V = \cos \theta_S + \frac{1}{2}\frac{\beta \varepsilon V^2}{\gamma d}, \tag{1b}$$

where β is the fraction of solid surface area contacting the liquid, θ_Y is the microscopically observed Young's contact angle as derived from only interfacial surface tension, θ_s is the macroscopically observed contact angle due to the effect of β, γ is the interfacial surface tension between the saline and the ambient environment, ε and d provide the capacitance of the hydrophobic dielectric, V is the applied dc or ac rms voltage, and θ_V is the macroscopically observed electrowetted contact angle. Equation (1b) in conjunction with the parameters described for fabrication of the PEN textile are plotted in Fig. 2. The measured initial contact angle is $\sim 10°$ lower than the theoretical value predicted by Eq. (1a). This is expected because the PEN textile exhibited $\sim 20°$ of contact angle hysteresis and since there is a temporary increase in droplet area during application of the droplet to the textile. For textile applications, this reduction in initial contact angle is likely representative of most liquid/textile encounters. The remainder of the experimental electrowetting response follows expected electrowetting behavior, including the typical onset of electrowetting saturation[4] at $\sim 70°$. The experimental contact angle reduction occurs at slightly lower voltages than theoretically predicted. This suggests that the dielectric capacitance or β are slightly different than that predicted by the fabrication criteria. Reversible electrowetting is achieved down to $\theta_V \sim 100°$. Irreversible wetting at $\theta_V \sim 100°$ indicates that the microscopic contact angle has reached the threshold for capillary wetting into the textile pores. We speculate that the controllable onset of capillary wetting through the textile might be the most promising capability for textile applications. Electrowetting behavior for the microfiber textile was also observed and plotted in Fig. 3. The highly irregular surface of the microfiber textile observed in Fig. 1(b) does not allow a direct calculation of β and contact angle according to Eq. (1b). However, as expected the increased roughness did result in a more hydrophobic initial contact angle of $\sim 130°$. Reversible electrowetting of the microfiber textile was not observed. This is expected since the irregular surface geometry of microfiber scaffold has numerous converging and diverging capillary features. Electrowetting into a converging capillary feature should occur at lower voltages and can lead to irreversible wetting. Electrowetting was tested to the limit of the voltage source and electrowetting saturation was not observed.

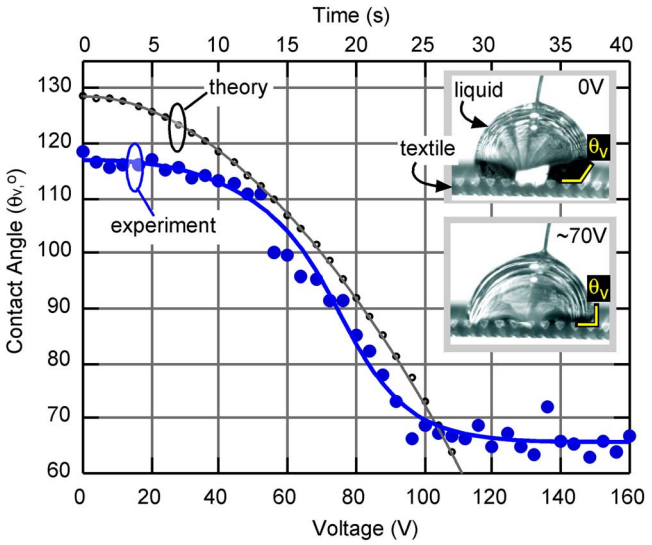


FIG. 2. (Color online) Theoretical and experimental electrowetting contact angles vs. voltage for the PEN textile. Also provided are photographs of the droplets at 0 and 70 V, and the time scale corresponding to the voltage ramp.

In previous work, we have demonstrated that using oil as the ambient allows full electrowetting reversibility on carbon

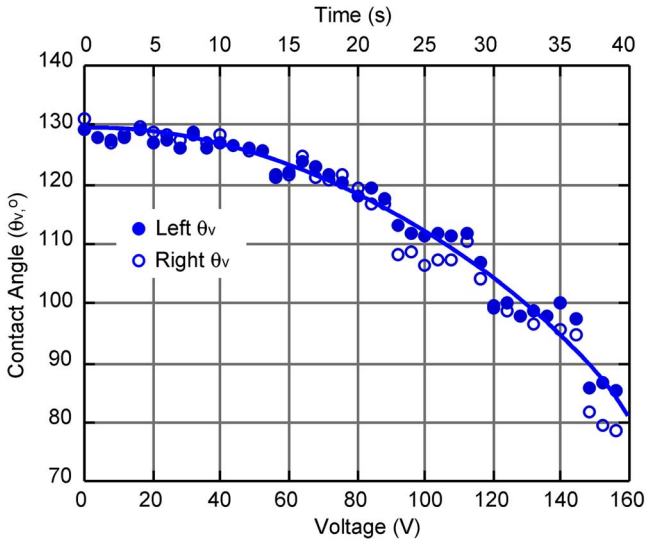


FIG. 3. (Color online) Electrowetting contact angle vs voltage for the microfiber textile. Both left and right side contact angles are provided since the microfiber textile surface was highly irregular. The time scale corresponding to the voltage ramp is also provided.

Downloaded 25 Jan 2008 to 129.137.215.236. Redistribution subject to AIP license or copyright; see http://apl.aip.org/apl/copyright.jsp

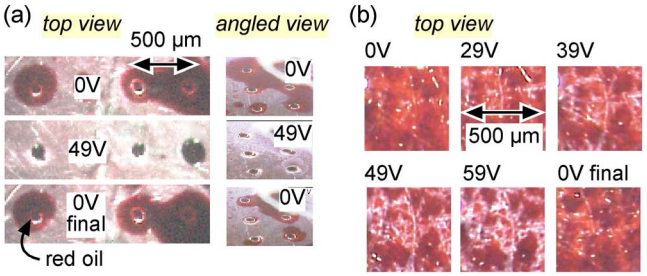


FIG. 4. (Color online) Optical images of water/dodecane:dye electrowetting on (a) PEN textiles and (b) microfiber textiles. For both experiments the textile is covered with, and imaged through, a continuous water layer.

nanofiber scaffolds.[19] Therefore, additional electrowetting experiments were performed using water and dodecane ($\gamma \sim 25$ mN/m) colored with a red nonpolar dye. In addition to improved electrowetting reversibility, the ability to use electrowetting to alter the color of the textile substrate might be of interest for applications such as electronic paper. Photographs during electrowetting were taken for both the PEN and microfiber textiles, and are shown in Fig. 4. The images in Fig. 4 are taken through a water layer that covers the oil film and textile. At zero voltage, Young's contact angle for the water exceeds 170° and the oil is spread thin over the surface with a complimentary oil contact angle of $<10°$. As voltage is increased, the water contact angle decreases, the oil contact angle increases, and the oil obtains a spherical cap geometry.[9] For the PEN textile shown in Fig. 4(a), the motion of the oil self-aligns to the pores in the textile. We are currently investigating the role of the radius of curvature of the oil meniscus below/above the textile (r) and the corresponding Young-Laplace pressure $\Delta p \propto 2\gamma/r$. These results will be reported in a future publication. The microfiber textile also exhibits a reduction in the oil area as applied voltage is increased and also exhibits reversible electrowetting [Fig. 4(b)]. The highly irregular surface of the microfiber textile makes formation of a predictive model challenging. However, from the photographs it is observed that the thinnest oil (lighter red) is generally the first to displace via electrowetting. It is speculated that these areas with thinner oil are topographically the flattest and/or are of higher relative elevation compared to surrounding textile areas.

The techniques demonstrated herein provide a means by which electrowetting can be integrated into film and fiber-based nonwoven textiles. With future development, electrowetting textiles might provide textile engineers with a new tool for creating applications where textile wetting is modulated at the end-user level. It is important to note that the higher voltages utilized herein can be lowered through addition of surfactants [lower γ, Eq. (1b)], and/or by narrowing the functionality of the textile to simple gating of capillary wetting. Such textiles might utilize converging capillaries and/or water with surfactant to create an initial contact angle that is near the threshold of capillary wetting. Therefore, according to Eq. (1b) only a small voltage ($\sim$10–20 V) would be required to induce liquid wetting into the textile. Also of interest in future work is integrating the second counter electrode within the textile, or providing the counter electrode as second textile in a two-ply format.

The Cincinnati authors acknowledge and thank D. O'Neill and M. Ludwig for their input and encouragement on this work.

[1] R. Rosario, D. Gust, M. Hayes, F. Jahnke, J. Springer, and A. A. Garcia, Langmuir **18**, 8062 (2002).
[2] D. S. Morton, R. S. Subramanian, and R. Balasubramaniam, Phys. Fluids A **2**, 2119 (1990).
[3] A. Diaz, P. A. Quintela, J. M. Schuette, and A. E. Kaifer, J. Phys. Chem. **92**, 3537 (1988).
[4] F. Mugele and J.-C. Baret, J. Phys.: Condens. Matter **17**, R705 (2005).
[5] M. G. Pollack, A. D. Shenderov, and R. B. Fair, Lab Chip **2**, 96 (2002).
[6] H. Moon, S. K. Cho, R. L. Garrell, and C.-J. Kim, J. Appl. Phys. **92**, 4080 (2002).
[7] B. Berge and J. Peseux, Eur. Phys. J. E **3**, 159 (2000).
[8] N. R. Smith, D. C. Abeysinghe, J. W. Haus, and J. Heikenfeld, Opt. Express **14**, 6557 (2006).
[9] R. A. Hayes and B. J. Feenstra, Nature (London) **425**, 383 (2003).
[10] J. Heikenfeld and A. J. Steckl, Appl. Phys. Lett. **86**, 011105 (2005).
[11] K. Natarajan, A. Dhawan, A. M. Seyam, T. K. Ghosh, and J. F. Muth, Mater. Res. Soc. Symp. Proc. **736**, 85 (2002).
[12] D. R. Bosak, A. A. Ogale, and J. Van Dun, Text. Res. J. **75**, 50 (2005).
[13] S. A. Harfenist, S. D. Cambron, E. W. Nelson, S. M. Berry, A. W. Isham, M. M. Crain, K. M. Walsh, R. S. Keynton, and R. W. Cohn, Nano Lett. **4**, 1931 (2004).
[14] M. Agarwal, Y. Lvov, and K. Varahramyan, Nanotechnology **17**, 5319 (2006).
[15] K. Varahramyan and Y. Lvov, J. Nanoeng. Nanosyst. **220**, 29 (2006).
[16] T. N. Krupenkin, J. A. Taylor, T. M. Schneider, and S. Yang, Langmuir **20**, 3824 (2004).
[17] D. L. Herbertson, C. L. Evans, N. J. Shirtcliffe, G. McHale, and M. I. Newton, Sens. Actuators, A **130-131**, 189 (2006).
[18] A. Torkelli, Helsinki University of Technology, Finland, VTT Technical Research Centre of Finland Publications (2003).
[19] M. S. Dhindsa, N. R. Smith, and J. Heikenfeld, Langmuir **22**, 9030 (2006).

Downloaded 25 Jan 2008 to 129.137.215.236. Redistribution subject to AIP license or copyright; see http://apl.aip.org/apl/copyright.jsp